AIP Advances

Thermotropic phase transitions in Pb1−x Sr x (Al1/3Nb2/3)0.1(Zr0.52Ti0.48)0.9O3 ceramics: Temperature dependent dielectric permittivity and Raman scattering

C. Q. Li, L. Peng, P. Wang, K. Jiang, A. Y. Liu, Z. G. Hu, and J. H. Chu

Citation: AIP Advances **5**, 067122 (2015); doi: 10.1063/1.4922439
View online: http://dx.doi.org/10.1063/1.4922439
View Table of Contents: http://scitation.aip.org/content/aip/journal/adva/5/6?ver=pdfcov
Published by the AIP Publishing

Thermotropic phase transitions in $Pb_{1-x}Sr_x(Al_{1/3}Nb_{2/3})_{0.1}(Zr_{0.52}Ti_{0.48})_{0.9}O_3$ ceramics: Temperature dependent dielectric permittivity and Raman scattering

C. Q. Li (李传青),[1] L. Peng (彭亮),[1] P. Wang (王鹏),[2] K. Jiang (姜凯),[1] A. Y. Liu (刘爱云),[2] Z. G. Hu (胡志高),[1,a] and J. H. Chu (褚君浩)[1]

[1]*Key Laboratory of Polar Materials and Devices, Ministry of Education, Department of Electronic Engineering, East China Normal University, Shanghai 200241, China*

[2]*Department of Physics, Shanghai Normal University, Shanghai 200234, China*

(Received 22 April 2015; accepted 30 May 2015; published online 8 June 2015)

The phase transitions of $Pb_{1-x}Sr_x(Al_{1/3}Nb_{2/3})_{0.1}(Zr_{0.52}Ti_{0.48})_{0.9}O_3$ (Sr-modified PAN-PZT) ceramics with Sr compositions of x = 2%, 5%, 10% and 15% have been investigated using X-ray diffraction (XRD), temperature dependent dielectric permittivity and Raman scattering. The XRD analysis show that the phase transition occurs between Sr composition of 5% and 10%. Based on the broad dielectric peaks at 100 Hz, the diffused phase transition from tetragonal (T) to cubic (C) structure shifts to lower temperature with increasing Sr composition. The dramatic changes of wavenumber and full width at half-maximum (FWHM) for $E(TO_4)'$ softing mode can be observed at morphotropic phase boundary (MPB). Moreover, the MPB characteristic shows a wider and lower trend of temperature region with increasing Sr composition. It could be ascribed to the diminishment of the energy barrier and increment of *A*-cation entropy. Therefore, the Sr-modified PAN-PZT ceramics unambiguously undergo two successive structural transitions (rhombohedral-tetragonal-cubic phase) with temperature from 80 to 750 K. Correspondingly, the phase diagram of Sr-modified PAN-PZT ceramics can be well depicted. [http://dx.doi.org/10.1063/1.4922439]

I. INTRODUCTION

In the past few decades, $Pb(Zr_{1-x}Ti_x)O_3$ (PZT) system has attracted much attention due to its excellent properties of ferroelectric, piezoelectric and pyroelectric, which can be used in the high-energy storage capacitors, infrared detectors, piezoelectric transducers and actuators.[1,2] The PZT belong to the family of ABO_3 perovskite-type structure.[3] The sublattice *A* is occupied by Pb ions and *B* sites consist of Zr/Ti ions. Correspondingly, numerous experimental and theoretical researchers change the structural sort of PZT by doping or mixing the congeneric elements at *A*- or *B*-site, which makes the changed material possess unique structure and physical properties.[4] For example, lanthanum (La) modification in the *A*-site was often used to induce a diffused phase transtion and enhance antiferroelectric phase.[5] Moreover, incorporation of Sn^{4+} in the *B*-site can make $Pb(ZrSnTi)O_3$ much easier in compositional tailoring and enhance the stability of ferroelectric region.[6] Therefore, it is necessary to investigate the effect of the *A*- or *B*-site synchronous modification for PZT ceramics structure and physical properties, which may be able to further broaden the application in designing optical communication system and other optoelectronic devices in the future.

[a]Author to whom correspondence should be addressed. Tel.: +86-21-54345150. Fax: +86-21-54345119. Electronic mail: zghu@ee.ecnu.edu.cn

The phase diagram of PZT system presents the information: for $x \leq 46\%$, the crystals show rhombohedral symmetry; the morphotropic phase boundary (MPB) corresponds to x=46%~52%, whereas for x>52%, crystals exhibit tetragonal to cubic phase transition around 650 K and possess remarkable relaxor ferroelectric character.[7–9] Recently, $Pb(Al_{1/3}Nb_{2/3})O_3$-$Pb(Zr_{0.52}Ti_{0.48})O_3$ (PAN-PZT) ceramic, which is located near the MPB of the PZT, has been recognized as a potential alternative for normal PZT because of its relatively high ε and great energy conversion and charge storage.[10,11] Composition adjustments PAN-PZT such as Sr modification were also utilized to obtain desired high dielectric permittivity and enhance the rhombohedral (R) to tetragonal (T) and tetragonal to cubic (C) phase transitions for $Pb_{1-x}Sr_x(Al_{1/3}Nb_{2/3})_{0.1}(Zr_{0.52}Ti_{0.48})_{0.9}O_3$ (Sr-modified PAN-PZT) ceramics. However, phase transition behaviors and ceramic properties during phase transitions in this composition based ceramics have been seldom reported.[12,13] No phase diagram was now available for Sr-modified PAN-PZT ceramics, which restricted the application of this ceramics system severely. In this article, we investigated the phase transition and low wavenumber phonon modes of Sr-modified PAN-PZT ($2.0\% \leq x \leq 15.0\%$) ceramics through X-ray diffraction (XRD), temperature dependent dielectric measurement and Raman scattering, which have an abnormal variation corresponding to the phase transition. The variations and physical origins of low wavenumber phonon modes have been discussed in detail.

II. EXPERIMENTAL DETAILS

The Sr-modified PAN-PZT ceramics were grown by traditional solid-state reaction sintering method. Stoichiometric mixture of analytical reagent grade powders PbO, ZrO_2, TiO_2, Al_2O_3, Nb_2O_5, ZnO and $SrCO_3$ were used as raw material. The sintering process was carried out in a lead rich environment in order to minimize lead volatilization. The samples were sintering at 1200 °C for 2 hour in air atmosphere. The ceramics with the diameter of 13 mm and the thickness of 1 mm were rigorously single-side polished. The structures of the Sr-modified PAN-PZT ceramics were investigated by XRD using a Ni filtered Cu-Kα radiation operated at 40 kV and 200 mA (D/MAX-2550V, Rigaku Co.). Temperature dependent dielectric permittivity ε was measured by HP4192 Impedance/Gain Phase analyzer from 300 K to 750 K with the heating rate of 2 K/min at 100 Hz, 1 kHz, 10 kHz and 100 kHz, respectively. The Raman scattering measurements were carried out by a Jobin-Yvon LabRAM HR 800 UV micro-Raman spectrometer and a THMSE 600 heating/cooling stage (Linkam Scientific Instruments) in the temperature range from 100 to 480 K with a resolution of 0.1 K. A laser with the wavelength of 633 nm was taken as the exciting source and the spectral resolution is better than 1 cm^{-1}. The laser beam was focused through a 50× microscope and the diameter of the laser spot is about 5 μm. An air-cooled charge coupled device (CCD) was used to collect the scattered signal dispersed on 1800 grooves/mm grating. To get rid of the trivial temperature dependence, all Raman spectra have been corrected by the Bose-Einstein occupation number $n(\omega) + 1 = 1/[1 - \exp(-\hbar\omega/k_BT)]$ ($\hbar$ and k_B are Planck constant and Boltzmann constant, respectively). In order to clarify the variation trend of each phonon modes, Raman spectra were fitted using independent damped harmonic oscillators. As we know, the Lorentz dispersion theory, which has physical meanings, can be constructed from the damped harmonic oscillator approximation, as compared to the Gaussian function. Moreover, the fitting model is widely acceptable and suitable for insulators and semiconductors.[14] To obtain the well-defined fitting quality, the Raman spectra were fitted using Lorentzian line shape approximation in the present work.

III. RESULTS AND DISCUSSION

Fig. 1(a) shows the XRD patterns of the Sr-modified PAN-PZT ceramics for the compositions with x=2%, 5%, 10% and 15% in the 2θ range of 20°-80° at room temperature. The strongest (110) diffraction peak is located at about 31°and other relatively weak peaks also appear. It indicates that the ceramics are pure perovskite phase and there is no secondary pyrochlore phase. The full width at half-maximum of the (100) peak with different Sr compositions are about 0.374°, 0.349°, 0.334° and 0.321°, respectively. From the each full width at half-maximum of the (100) peak, the grain size

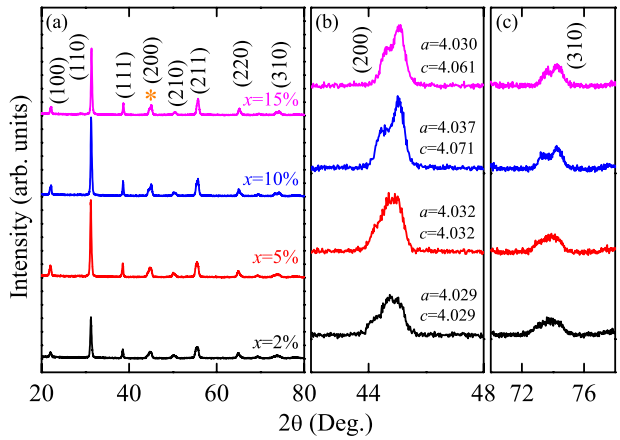

FIG. 1. (a) The XRD pattern of the Sr-modified PAN-PZT ceramics with different Sr composition. The label (∗) indicates the (200) peak in the rhombohedral phase, which splits to (002) and (200) peak in the tetragonal phase. Note that x (x=2%, 5%, 10% and 15%) represents different Sr compositions. (b) and (c) The enlarged region for the diffraction peaks at $2\theta \approx 45^{\circ}$ and 74°, respectively. Note that the unit of the lattice parameter is Å.

of the four samples are about 22 nm, 23 nm, 25 nm and 26 nm, respectively, which estimated by the Scherrer formula [$D = 0.89\lambda/(\beta \cos\theta)$]. Because the difference between the lattice parameter a and c in tetragonal lattice system, it is known that the peak splits at $2\theta \approx 45°$ when the transition occurs from R to T phase. The phenomena could be clearly observed in the enlarged patterns of Fig. 1(b) and 1(c). For the compositions with x=2% and 5% there is no splitting, whereas the compositions with x=10% and 15%, the (200) peak splits into rhombohedral (200) and tetragonal (002) while the (111) peak is a singlet, which is similar to the $(1-x)Pb(Mg_{1/3}Nb_{2/3})O_3-xPbTiO_3$ piezoelectric ceramics,[15–18] suggesting that introduction of Sr ions induce the conversion of R to T phase. Meanwhile, we can see the asymmetric shoulder towards to a higher 2θ side is resulted from the fact that the ionic radius of Sr^{2+} (1.18 Å) is smaller than that of Pb^{2+} (1.49 Å) inducing distortion and reducing the cell volume with shortened a-axis and c-axis in the perovskite structure.[19] The lattice parameters were listed in Fig. 1(b). The value of a increases from 4.029 Å to 4.032 Å in the rhombohedral structure for the Sr composition of less than 5%. The similar augment could be recognized in the value of c for the rhombohedral structure, while the parameter a and c decrease for tetragonal structure. However, the c/a ratio value increases when the conversion occurs from rhombohedral to tetragonal structure, which is similar to $Pb(Zn_{1/3}Nb_{2/3})O_3$-$Pb(Zr_{0.55}Ti_{0.45})]O_3$ system.[20] It should be emphasized that an evident variation of the c/a ratio value is often associated with the occurrence of phase transition. Thus, one can expect that there will be different spectral response for the Sr-modified PAN-PZT ceramics with the R and T phase, respectively.

Fig. 2 illustrates the ε as a function of temperature for different Sr-modified PAN-PZT ceramics at 100 Hz, 1 KHz, 10 KHz and 100 KHz, respectively. One dielectric anomaly can be observed for all Sr compositions at various frequencies, which is designated as Curie temperature (T_C), where the ε reaches its maximum. It is worth noting that there is only one obvious broad peak located at T_C for each dielectric spectrum, indicating that the solid solutions possess a certain dielectric relaxors, which corresponds to transition from ferroelectric to paraelectric. From the inset of Fig. 2, we can see the T_C was shifted to lower temperature and the values of the dielectric maxima (ε_m) increase then decrease with increasing Sr composition. The reason of this decline in T_C was due to the existence of heterogeneous templates ($SrCO_3$) and the decrease in tetragonality (c/a).[21,22] Besides, the diffused phase transition process characterized by the broad dielectric peaks can be well observed for increasing Sr composition. That is because Sr addition induces the interaction of the ferroelectric and paraelectric. The orgin of the relaxor behavior is connected with the dynamic behavior and temperature evolution of nano-regions with the compositionally disordered crystals.[23] Furthermore, the width of ε was found to be broader with increasing Sr composition, suggesting a stronger relaxor behavior.

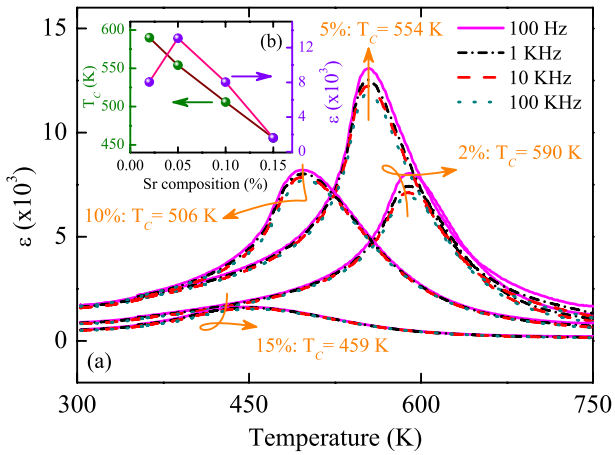

FIG. 2. Temperature dependence of dielectric constant (ε) for different Sr-modified PAN-PZT ceramics at 100 Hz, 1 KHz, 10 KHz and 100 KHz, respectively. The inset show the evolutions of the Curie temperature (T_C) and the maximum for ε with all Sr composition at 100 Hz.

Theoretically, in high temperature cubic paraelectric phase space group $Pm3m$ (O_h) of Sr-modified PAN-PZT ceramics with five atoms per unit cell, there are 12 optical vibration phonon modes transform as the $3T_{1u} + T_{2u}$ irreducible representation.[24,25] In the ferroelectric rhombohedral with space group $R3m(C_{3v})$ and tetragonal space group $P4mm(C_{4v})$ structures of the Sr-modified PAN-PZT ceramics, each triply degenerate T_{1u} mode splits as A_1+E and the silent T_{2u} mode as B_1+E mode. Fig. 3(a) depicts room-temperature Raman spectra and well-fitted deconvolution peaks for all Sr-modified PAN-PZT ceramics. The four spectra have similar profiles and all the phonon mode assignments at room temperature are listed in Table I. Compared with the relaxor PZT and $(Pb_{1-1.5x}La_x)(Zr_{0.42}Sn_{0.40}Ti_{0.18}O_3$ (PLZST) ceramics,[5,14] the present results match well with the R phase of PZT and/or PLZST, which show sharp peaks at low wavenumbers. It should be emphasized that the assigned modes are necessary to reasonably interpret the variation of Raman spectra, where the some broadening peaks appear.[26] There are two peaks assigned as $E(TO_4)$ mode, stemming from the T_{1u} mode in the cubic phase, arising from the internal BO_6 bending modes.[14] Similar to the $E(TO_4)$ mode, the split $E(TO_2)$ is considered as the atom disorder of B-site cations. The peak shift indicates that due to the substitution of Sr^{2+} cation for Pb^{2+}, the strength of average B-O interactions becomes weaker. Thus, the phase transition in perovskite oxide system may be also changed.

To obtain the effect of temperature on thermotropic phase transitions, temperature dependence of experimental Raman spectra for Sr-modified PAN-PZT ceramics from 80 to 480 K were plotted in Figs. 3(b)-3(e). As it can be seen, the Raman spectra are typically relaxor ferroelectrics, showing

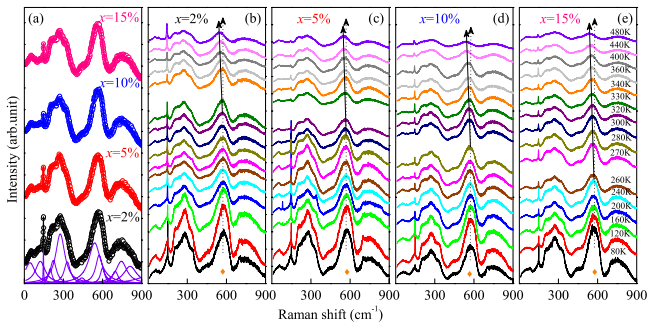

FIG. 3. (a) Raman spectra of different Sr-modified PAN-PZT ceramics at room temperature and the corresponding harmonic oscillator fitting results. (b)-(e) Temperature dependence of experimental Raman spectra for all Sr-modified PAN-PZT ceramics from 80 to 480 K. The symbols (♦) indicate the $E(TO_4)'$ phonon mode. The solid and dash lines are applied to guide the eyes.

TABLE I. The assignments of symmetries from the fitting deconvolution peaks in Raman scattering of Sr-modified PAN-PZT ceramics recorded at room temperature. Note that the unit of the phonon wavenumber is cm^{-1}.

	Phonon modes											
Samples	A_1 (TO_1)	A_1 (LO_1)	E(TO_2)	E(TO_2)′	A_1 (TO_2)	A_1 (LO_2)	E(TO_4)	E(TO_4)′	A_1 (TO_3)′	E(LO_3)	A_1 (LO_3)	Oxygen breathing
x=2.0%	146.2	197.8	222.1	275.1	328.7	440.8	538.8	573.6	599.4	696.4	744.0	811.5
x=5.0%	146.0	197.0	221.0	273.2	327.2	443.4	536.4	570.5	595.4	698.7	746.3	808.4
x=10.0%	146.3	198.3	224.6	271.8	324.3	444.6	539.1	571.8	595.7	702.3	750.7	817.0
x=15.0%	146.8	192.4	212.7	271.0	328.3	446.9	536.9	569.0	594.0	703.1	749.8	812.9

a number of broad bands.[18] Note that the relative intensities of Raman modes for all samples decrease with increasing temperature. One dominant feature is the decreasing of the intensities for the mode $E(TO_2)'$ (~275 cm^{-1}) and $E(TO_4)'$ (~573 cm^{-1}). As can be seen from Fig. 4(a)-4(d), the temperature dependence $E(TO_2)'$ intensity have a marked change near 340 K, 330 K, 300 K and 270 K with different Sr compositions, which are corresponding to R to T transition temperature. The phenomena are similar systems $(1-x)Pb(Mg_{1/3}Nb_{2/3})O_3$-$xPbTiO_3$.[15,17,18,27] Meanwhile, wavenumber shifting, mode merging and broadening are observed, which are typical for perovskite relaxor ferroelectrics.[28] For example, Figs. 3(b)-3(e) show apparent wavenumber shifts at about 340 K, 330 K, 300 K and 270 K for the mode $E(TO_4)$ (labeled as "*diamonds*") with increasing temperature, respectively. The structure of Sr-modified PAN-PZT ceramics transforms from R to T phase. The successive phase transitions in Sr-modified PAN-PZT ceramics derive from competition between soft phonon modes and relaxation modes. Also, the two peak shifts become noticeable with Sr components by comparing solid arrows with dot arrows, and the splitting peaks are clearer in the wavenumber range of 150~400 cm^{-1} and 500~650 cm^{-1}. For a closer inspection, the mode $E(LO_2)$ (~222 cm^{-1}) has a clear red-shift in the wave number position and merges into the adjacent mode when transformation from R to T phase occurs. While the mode A_1 (LO_2) (~328 cm^{-1}) exhibits blue-shift and has a tendency to merge into the mode at 275 cm^{-1}, indicates the mode anomalously harden with temperature from R to T phase across the successive transitions. From the point of view of symmetry structure transition with temperature, the point group also belongs to C_{3v} to C_{4v} transition. This can be demonstrated by the behavior of red-shift and broadening of the mode at

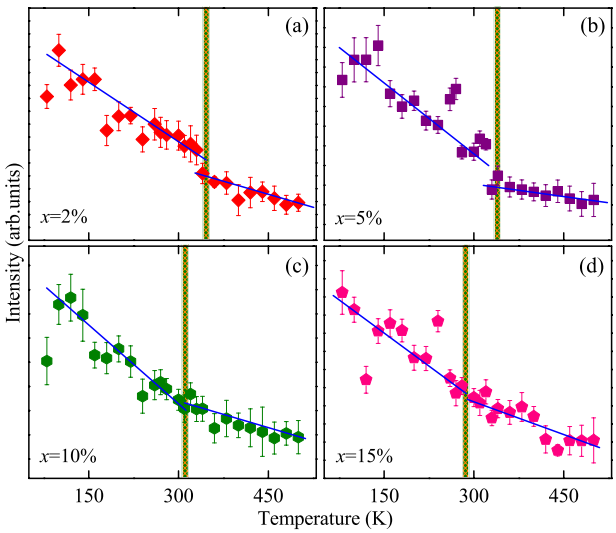

FIG. 4. (a)-(d) Temperature dependence of intensity from the mode E(TO_2)′ (~275 cm^{-1}) of the PAN-PZT ceramics with different Sr compositions. Note that the shades represent the phase transition temperature.

573 cm^{-1}. It is known that the mode numbers between the experiment and theoretical analysis of Raman modes are slightly different. This discrepancy of the Raman mode numbers can be explained by the existence of the polar nanoregions.[29]

To depict thermal evolution of low wavenumber phonon modes at all temperature below T_C, the temperature dependence of the wavenumber and full width at half-maximum (FWHM) from $E(TO_4)'$ mode are plotted in Fig. 5(a)-5(d). A similar remarkable variation of wavenumber shift and FWHM could be observed for the four samples at the temperature of about 340 K, 330 K, 300 K and 270 K, respectively. Suggesting that the R to T phase transition occurs obviously, which is corresponding to mode softening with temperature in each phase and exactly as expected to follow from the lattice thermal expansion. Note that the phase transition regions (R+T) can be easily recognized based on the abrupt variations with increasing temperature. Furthermore, it is quite clear that the region is wider and shifts to lower temperature as increasing the doping of Sr, which can be explained by the coexistence region inversely proportional to the grain size of modified materials. For example, the smaller ionic radius of La^{3+} (1.36 Å) and Nd^{3+} (0.98 Å) substitute for Pb^{2+} (1.49 Å) in the *A*-cation sites in PZT, can shift the MPB and increase the width of the coexistence region.[30] Thus, the phase transition zone of the Sr-doped PAN-PZT ceramics can also be widened because of the smaller ionic radius of Sr^{2+} (1.18 Å) than Pb^{2+}. From Fig. 5(a)-5(d), the phase transition widths of the Sr-modified PAN-PZT ceramics can be roughly estimated to 50 K, 80 K, 125 K and 155 K, corresponding to increasing the doping of Sr. These values are similar to PLZST ceramics and slightly larger than those for $Pb_{0.5}Sr_{0.5}TiO_3$ films derived from refractive index.[5,31]

Based on the temperature dependent dielectric permittivity and the variations of wavenumber, intensity and FWHM for $E(TO_4)'$ phonon modes, the phase diagram of Sr-modified PAN-PZT ceramics can be presented in Fig. 5(e). The phase diagram can be divided into three parts, with T phase existing between R and C phases. At room temperature, the Sr-modified PAN-PZT ceramic goes through a transformation from R to T phase when the composition of Sr exceeds 10%, which is consistent with the XRD results mentioned previously. Furthermore, the samples undergo successive phase transitions as increasing temperature. For Sr-modified PAN-PZT with x=2%, when the temperature increases the R to T phase transition occurs at 340 K. Meanwhile, from the temperature

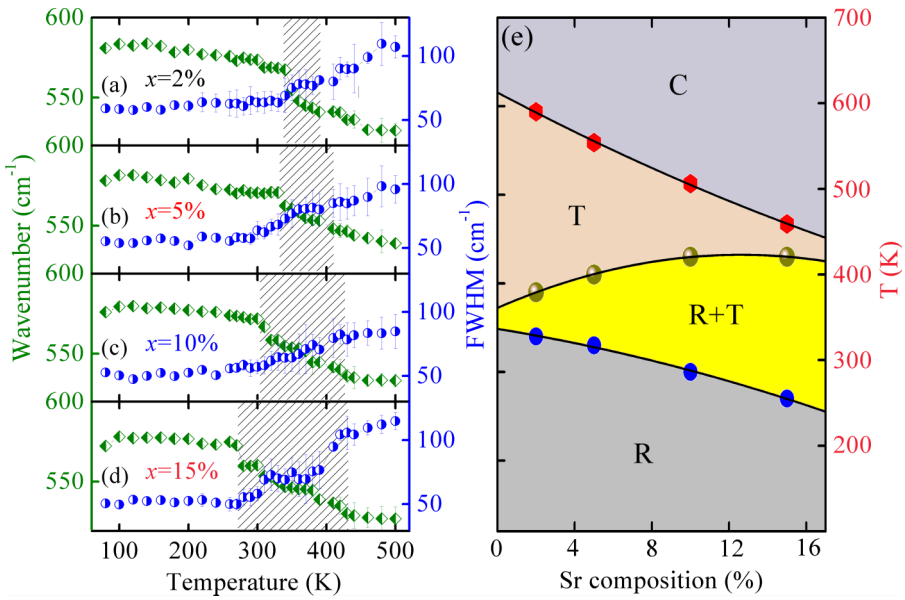

FIG. 5. (a)-(d) Temperature dependence of $E(TO_4)'$ mode wavenumber and FWHM from all the Sr composition. Note that the shadow pattern indicates the MPB region, which is different with increasing Sr composition. (e) The phase diagram of Sr-modified PAN-PZT ceramics based on the low wavenumber phonon mode variations with temperature and Sr composition. The phase transition regions of rhombohedral (R), tetragonal (T) and cubic (C) characteristics can be clearly distinguished by the solid dots.

dependence of ε we can see the T ferroelectric to C paraelectric phase transformation occurs at T_C=590 K. From the phase diagram, one can see that the R to T and T to C phase transition temperature decreases and the phase transition regions are widened as increasing the composition of Sr. Note that the boundaries in the phase diagram should not be taken rigorously. It is because the phase coexistence may occur over a relatively wide temperature region.

IV. SUMMARY

In summary, temperature dependence of the phonon wavenumbers through the successive thermotropic phase transitions has been reported. With increasing Sr composition, the transition temperature region, at which rhombohedral to tetragonal, becomes wider and lower. The diffused phase transition from ferroelectric to paraelectric shifts to lower temperature.

ACKNOWLEDGMENTS

One of the authors (C. Q. Li) would like to thank Dr. Xuefeng Chen, Jinzhong Zhang, and Jiajun Zhu for constructive discussions. This work was financially supported by Major State Basic Research Development Program of China (Grant Nos. 2011CB922200 and 2013CB922300), Natural Science Foundation of China (Grant Nos. 11374097 and 61376129), Projects of Science and Technology Commission of Shanghai Municipality (Grant Nos. 14XD1401500, 13JC1402100 and 13JC1404200), and the Program for Professor of Special Appointment (Eastern Scholar) at Shanghai Institutions of Higher Learning.

[1] A. S. Mischenko, Q. Zhang, J. F. Scott, R. W. Whatmore, and N. D. Mathur, Science **311**, 1270 (2006).
[2] M. Ahart, M. Somayazulu, R. E. Cohen, P. Ganesh, P. Dera, H. K. Mao, R. J. Hemley, Y. Ren, P. Liermann, and Z. Wu, Nature **451**, 545 (2008).
[3] M. Suewattana and D. J. Singh, Phys. Rev. B. **73**, 224105 (2006).
[4] B. Mihailova, B. Maier, C. Paulmann, T. Malcherek, J. Ihringer, M. Gospodinov, R. Stosch, B. Güttler, and U. Bismayer, Phys. Rev. B. **77**, 174106 (2008).
[5] X. Chen, Z. G. Hu, Z. H. Duan, X. F. Chen, G. S. Wang, X. L. Dong, and J. H. Chu, J. Appl. Phys. **114**, 043507 (2013).
[6] N. Luo, Y. Li, Z. Xia, and Q. Li, CrystEngComm. **14**, 4547 (2012).
[7] B. Noheda, D. E. Cox, G. Shirance, J. A. Gonzalo, L. E. Cross, and S-E. Park, Appl. Phys. Lett. **74**, 2059 (1999).
[8] B. Noheda, D. E. Cox, G. Shirance, R. Guo, B. Jones, and L. E. Cross, Phys. Rev. B. **63**, 014103 (2001).
[9] B. Jaffe, W. R. Cook, and H. Jaffe, *Piezoelectric Ceramics* (Academic, London, 1971).
[10] L. L. Wei, A. Y. Liu, C. C. Jin, F. T. Lin, P. Wang, Q. R. Yao, C. Y. Tian, Y. Li, J. Tang, H. L. Han, W. Z. Shi, and C. B. Jing, J. Alloys. Compd. **590**, 368 (2014).
[11] J. Y. Lee, J. W. Choi, M. G. Kang, S. J. Kim, T. K. Ko, and S. J. Yoon, J. Electroceram. **23**, 572 (2009).
[12] Z. H. Dai, Z. Xu, and X. Yao, Appl. Phys. Lett. **92**, 072904 (2008).
[13] L. Shebanov, M. Kusnetsov, and A. Sternberg, J. Appl. Phys. **76**, 4301 (1994).
[14] E. Buixaderas, M. Berta, L. Kozielski, and I. Gregora, Phase Transitions. **84**, 528 (2011).
[15] M. P. Thia, G. Marchb, and P. Colombanb, J. Eu. Ceramic. Soc. **25**, 3335 (2005).
[16] M. P. Thia, H. Hemery, P. Colombanb, and O. Lacour, in *2004 14th IEEE International Symposium on the Applications of Ferroelectrics-ISAF-04*, *Montreal, Canada*, *23-27 August 2004*. pp. 157-160.
[17] G. Gouadec, P. Colomban, A. Slodczyk, and M. P. Thi, in Joint IEEE international Symposium on the Applications of Ferroelectrics, International workshop on Acoustic Transduction Materials and Devices & Workshop on Piezoresponse Force Microscopy (ISAF/IWATMD/PFM), Penn State University in State College, PA, USA, 12-16 May 2014.
[18] A. Slodczyk, G. Gouadec, P. Colomban, and M. P. Thi, in *Joint UFFC, EFTF and PFM Symposium*, *Prague, Czech Republic*, *21-25 July 2013*. pp. 356-359.
[19] Y. H. Xu, *Ferroelectrics and Piezoelectric Materials* (Science Press, 1978).
[20] X. Zeng, X. Y. He, W. X. Cheng, X. S. Zheng, and P. S. Qiu, J. Alloys. Compd. **485**, 843 (2009).
[21] M. R. Suchomel and P. K. Davies, Appl. Phys. Lett. **86**, 262905 (2005).
[22] J. Kelly, M. Leonard, C. Tantigate, and A. Safari, J. Am. Ceram. Soc. **80**, 957 (1997).
[23] A. Kumar, I. Rivera, and R. S. Katiyar, J. Raman Spectrosc. **40**, 459 (2009).
[24] M. Deluca, H. Fukumura, N. Tonari, C. Capiani, N. Hasuike, K. Kisoda, C. Galassi, and H. Harima, J. Raman Spectrosc. **42**, 488 (2011).
[25] G. Burns and B. A. Scott, Phys. Rev. B. **7**, 3088 (1973).
[26] E. Buixaderas, V. Bovtun, S. Veljko, M. Savinov, P. Kužel, I. Gregora, S. Kamba, and I. Reaney, J. Appl. Phys. **108**, 104101 (2010).
[27] A. Slodczyk and P. Colomban, Materials. **3**, 5007 (2010).
[28] M. Shen, G. G. Siu, Z. K. Xu, and W. Cao, Appl. Phys. Lett. **86**, 252903 (2005).
[29] M. El Marssi and H. Dammak, Solid State Commun. **142**, 487 (2007).
[30] J. Frantti, V. Lantto, and J. Lappalainen, J. Appl. Phys. **79**, 1065 (1996).
[31] M. Tyunina, A. Dejneka, D. Chvostova, J. Levoska, M. Plekh, and L. Jastrabik, Phys. Rev. B. **86**, 224105 (2012).